© 2016. Published by The Company of Biologists Ltd | Journal of Cell Science (2016) 129, 3770-3780 doi:10.1242/jcs.189332

RESEARCH ARTICLE

Cdc48 and Ubx1 participate in a pathway associated with the inner nuclear membrane that governs Asi1 degradation

Marina Pantazopoulou[1], Mirta Boban[2], Roland Foisner[3] and Per O. Ljungdahl[1,*]

ABSTRACT

The nuclear envelope is a barrier comprising outer and inner membranes that separate the cytoplasm from the nucleoplasm. The two membranes have different physical characteristics and protein compositions. The processes governing the stability of inner nuclear membrane (INM) proteins are not well characterized. In *Saccharomyces cerevisiae*, the INM Asi1–Asi3 complex, principally composed of integral membrane proteins Asi1 and Asi3, is an E3 ubiquitin ligase. In addition to its well-documented function in endoplasmic reticulum (ER)-associated degradation, the Doa10 E3 ubiquitin ligase complex partially localizes to the INM. The Asi1–Asi3 and Doa10 complexes define independent INM-associated degradation (INMAD) pathways that target discrete sets of nuclear substrates for proteasomal degradation. Here, we report that Asi1 is rapidly turned over ($t_{1/2}$≤30 min). Its turnover depends on ubiquitin-mediated degradation by nucleus-localized proteasomes, exhibiting a clear requirement for the E2 ubiquitin-conjugating enzyme Ubc7, Cue1 and the AAA ATPase Cdc48 and co-factor Ubx1. Asi1 turnover occurs largely independently of the Asi1–Asi3 or Doa10 complexes, indicating that it is subject to quality control at the INM in a manner distinct from that of the characterized INMAD pathways.

KEY WORDS: Nuclear envelope, Ubiquitin, Proteasome, Inner-nuclear-membrane-associated degradation, INMAD, Membrane dislocation, *Saccharomyces cerevisiae*

INTRODUCTION

The nuclear envelope comprises the outer nuclear membrane (ONM) and the inner nuclear membrane (INM). These two membranes are continuous but functionally separated by nuclear pore complexes (NPCs) anchored in the bridging membranes. In addition to providing the main route of soluble transport in and out of the nucleus, NPCs provide a physical barrier that must be overcome for the movement of membrane proteins from the ONM to INM. Consequently, the nuclear membranes have unique properties and protein compositions. The endoplasmic reticulum (ER) extends directly from the ONM, and thus, the ONM and ER are quite similar. By contrast, the composition of the INM is not well established. However, proteins localized to the INM are known to participate in a variety of essential cellular processes, including maintenance of the nuclear architecture, transcriptional regulation, chromatin organization and DNA repair (Heessen and Fornerod, 2007; Mekhail and Moazed, 2010).

The diverse protein quality control pathways in eukaryotic cells share the common feature of orchestrating the attachment of small protein tags to substrate proteins that function as targeting motifs for degradation. The most commonly used tag is ubiquitin (Varshavsky, 2012). Short-lived proteins, misfolded or damaged proteins, or functional proteins subject to downregulation are ubiquitylated by the sequential action of an E1 ubiquitin-activating enzyme, E2 ubiquitin-conjugating enzymes (Ubc) and E3 ubiquitin ligases. The reiteration of these enzymatic events leads to the polyubiquitylation of substrate proteins. Polyubiquitylated substrate proteins are targeted to one of two proteolytic compartments, either the vacuole (analogous to lysosomes of mammalian cells) or proteasomes. Vacuoles primarily receive degradation substrates through vesicle-mediated transport (Bryant and Stevens, 1998; Rendueles and Wolf, 1988). Proteasomes are large multicomponent proteases that assemble in the cytoplasm and nucleoplasm (Ciechanover, 2007; Hershko and Ciechanover, 1998).

Two ER-associated degradation (ERAD) complexes in yeast, named after their core E3 ligases Hrd1 and Doa10, respectively, represent well-characterized protein quality control systems that target misfolded ER and cytoplasmic proteins for degradation by cytoplasmic proteasomes (Carvalho et al., 2006; Denic et al., 2006; Hiller et al., 1996; Sommer and Jentsch, 1993; Werner et al., 1996). Hrd1 primarily operates with Ubc7, whereas Doa10 functions with both Ubc6 and Ubc7 (Bays et al., 2001; Plemper et al., 1999; Rubenstein et al., 2012; Swanson et al., 2001). Ubc6 is a C-terminal-tail-anchored membrane protein, whereas Ubc7 is recruited to the membranes through interactions with Cue1, a type-1 transmembrane protein (Biederer et al., 1997). In *cue1*Δ mutants, Ubc7 is targeted for proteasomal degradation by the action of the Ufd4 E3 ubiquitin ligase (Ravid and Hochstrasser, 2007). Ubc6 is itself a substrate for Doa10- and Ubc7-dependent ubiquitylation (Kreft and Hochstrasser, 2011; Swanson et al., 2001; Walter et al., 2001).

In addition to endogenous resident INM proteins, many membrane proteins that normally reside in other intracellular locations are apparently able to gain access to the INM by leaking past nuclear pore complexes (Foresti et al., 2014; Khmelinskii et al., 2014; Popken et al., 2015). Both resident and mislocalized INM proteins are subject to turnover (Khmelinskii et al., 2014; Omnus and Ljungdahl, 2014). Currently, two quality control pathways are known to operate in association with the INM in yeast (Deng and Hochstrasser, 2006; Foresti et al., 2014; Khmelinskii et al., 2014). Analogous to the ERAD complexes, the INM-associated degradation (INMAD) complexes are defined by their core E3 ubiquitin ligases. In addition to its well-established role in ERAD, Doa10 is able to pass the barrier of NPCs and function together with Ubc6 and Ubc7 in the INM to ubiquitylate multiple nuclear substrates, targeting them to nuclear proteasomes for degradation (Boban et al., 2014; Deng and Hochstrasser, 2006; Furth et al., 2011; Ravid et al., 2006). The

[1]Department of Molecular Biosciences, The Wenner-Gren Institute, Stockholm University, Stockholm SE-106 91, Sweden. [2]University of Zagreb, School of Medicine, Croatian Institute for Brain Research, Šalata 12, Zagreb 10000, Croatia. [3]Max F. Perutz Laboratories, Department of Medical Biochemistry, Medical University of Vienna, Dr. Bohr-Gasse 9, Vienna A-1030, Austria.

*Author for correspondence (per.ljungdahl@su.se)

P.O.L., 0000-0002-6625-3540

Received 15 March 2016; Accepted 18 August 2016

Journal of Cell Science (2016) 129, 3770-3780 doi:10.1242/jcs.189332

second, and most recently characterized, INMAD pathway is defined by the Asi1–Asi3 E3 ubiquitin ligase complex (Khmelinskii et al., 2014).

Asi1, Asi2 and Asi3 were originally identified based on their functions as negative regulators of the Ssy1–Ptr3–Ssy5 (SPS) nutrient-sensing pathway in yeast (Forsberg et al., 2001; Ljungdahl and Daignan-Fornier, 2012). Asi1 and Asi3 are homologous proteins: Asi1 (624 residues) and Asi3 (669 residues) are 31% identical and 42% similar in their sequences (Boban et al., 2006; Forsberg et al., 2001; Zargari et al., 2007). Both proteins have two equally sized domains – an N-terminal domain with five hydrophobic segments and a nucleoplasmically oriented hydrophilic C-terminal domain with a conserved Zn^{2+}-binding RING motif. Asi1 and Asi3 function together as components of the heterodimeric E3 ubiquitin ligase complex; the RING motifs of Asi1 and Asi3 interact with Ubc7 and Ubc6, respectively (Khmelinskii et al., 2014). Asi2 appears to function as a specificity factor or as an adaptor protein required for targeting substrates for Asi1–Asi3-dependent ubiquitylation (Khmelinskii et al., 2014). All three Asi proteins are required to catalyze the ubiquitylation of Stp1 and Stp2, the effector transcription factors of the SPS sensing pathway, when they inappropriately gain access to the nucleus in the absence of amino-acid-mediated induction (Khmelinskii et al., 2014; Omnus and Ljungdahl, 2014).

The Asi1–Asi3 complex ubiquitylates multiple integral membrane proteins when they mislocalize to the nuclear compartment (Foresti et al., 2014; Khmelinskii et al., 2014). Consistently, cells require a functional Asi1–Asi3 E3 ubiquitin ligase complex when misfolded proteins accumulate in the ER, a condition that presumably results in enhanced levels of mislocalized proteins in the INM. Strains carrying mutations in *HRD1* and *IRE2*, with compromised ERAD and unfolded-protein response pathways, respectively, exhibit impaired growth at elevated temperatures (Friedlander et al., 2000). The introduction of an *asi1*Δ allele into an *hrd1*Δ *ire1*Δ strain results in synthetic lethality (Foresti et al., 2014). These finding indicate that the protein quality control activity of the Asi1–Asi3 INMAD E3 ubiquitin ligase is essential for cells to maintain and safeguard the integrity of the nuclear compartment.

The processes governing the intrinsic stability of endogenous INM proteins are not well established. To fill the gap in knowledge, we have used the Asi proteins as model INM proteins to identify the cellular components that determine their stability. Here, we report that Asi1 is degraded rapidly within the nucleus, and we identify several cellular components required for its degradation. Intriguingly, Asi1 turnover occurs largely independent of the two known INMAD E3 ubiquitin ligase complexes, Asi1–Asi3 and Doa10. The results indicate that the INM possesses additional and previously unidentified protein quality control systems, a finding that has important implications for understanding the diverse functions associated with this vital intracellular membrane.

RESULTS

Asi1 and Asi3 exhibit rapid and independent rates of turnover

The stability of Asi1 and Asi3 carrying the indicated number of hemagglutinin (HA) epitope tags at their C-termini was determined in the presence of translation inhibitor cycloheximide (CHX) (Fig. 1). Protein levels were analyzed by immunoblotting for HA. Asi1 (Asi1–3HA, pPL1141) exhibited a half-life of approximately 30 min (Fig. 1A); chromosomal Asi1–3HA exhibited similar turnover rates (data not shown). Asi3–6HA (chromosomal) was more stable with a half-life of greater than 90 min (Fig. 1B). We examined whether the different rates of turnover affected the steady-state levels of Asi1 and Asi3 expressed from in-locus endogenously promoted genes encoding Asi1–6HA and Asi3–6HA (Fig. 1C). Consistent with a more-rapid turnover, the steady-state levels of Asi1–6HA (chromosomal) were significantly lower than those for Asi3–6HA (chromosomal). We then tested whether Asi3 and Asi2 affected Asi1 turnover. The data indicate that Asi1 turnover is independent of both Asi2 and Asi3 (Fig. 1D). Based on this and previous data examining the turnover of Asi2 (Boban et al., 2014), it is clear that each of the Asi proteins exhibits unique turnover kinetics.

Asi1 degradation occurs independently of SPS sensor signaling

The Asi proteins have been identified as negative regulators of the SPS sensing pathway that are required to suppress gene expression in the absence of amino-acid-mediated induction (Boban et al., 2006; Forsberg et al., 2001; Zargari et al., 2007). We tested the possibility that Asi1 becomes targeted for downregulation in an SPS-sensor-dependent manner. The stability of Asi1 was examined in cells lacking Ssy5, the endoprotease component of the SPS sensor. In *ssy5*Δ cells, Stp1 and Stp2 cannot be proteolytically activated, and hence, cells are insensitive to induction by extracellular amino acids. The rate of Asi1 degradation remained the same, independent of Ssy5 (Fig. 1E); a result consistent with our previous finding that Asi2 degradation occurs independently of SPS sensor signaling (Boban et al., 2014). Thus, the activity of the plasma-membrane-localized SPS sensor does not appear to influence the stability and turnover of the Asi proteins.

Asi1 is ubiquitylated and targeted for proteasomal degradation

We sought to define whether Asi1 turnover occurs in the vacuole or is proteasome dependent. First, we examined the stability of Asi1 in a *pep4*-null mutant strain with greatly diminished capacity to degrade vacuolar substrates (Ammerer et al., 1986; Woolford et al., 1986). Our results indicate that Asi1 degradation occurs independently of Pep4 (Fig. 2A); Asi1 exhibited similar stability in *PEP4* and *pep4*Δ strains, indicating that Asi1 is not degraded in the vacuole. Next, we assessed whether Asi1 is turned over in a proteasome-dependent manner. Asi1 stability was assessed in *cim3-1* mutants carrying temperature-sensitive mutations in *RPT6*, which encodes one of the ATPases present in the heterohexameric Rpt ring of the 19S regulatory particle of the proteasome (Ghislain et al., 1993; Schork et al., 1995). At non-permissive temperatures, the proteasomes of *cim3-1* mutants exhibit greatly impaired degradative capacity. Consistent with being a proteasome substrate, Asi1 exhibited clearly enhanced stability when expressed in a *cim3-1* mutant growing at the non-permissive temperature (Fig. 2B).

Most proteasomal substrates commonly require modification by polyubiquitin chains that act as a targeting signal recognized by the subunits of the 19S regulatory particle and additional shuttling receptors associated with the holo 26S proteasome (Chau et al., 1989; Ravid and Hochstrasser, 2008; Thrower et al., 2000). To examine the ubiquitylation status of Asi1, we performed immunoprecipitation experiments in cells overexpressing ubiquitin. Immunoblots for ubiquitin showed that the immunoprecipitated HA-tagged Asi1 is polyubiquitylated (Fig. 2C). Taken together, these observations suggest that the ubiquitin–proteasome system (UPS) dictates the stability of Asi1.

Asi1 is degraded by proteasomes that are localized to the nuclear compartment

Immuno-electron microscopy studies have clearly shown that the vast majority of Asi1 (>80%) is localized to the INM (Boban et al.,

Journal of Cell Science (2016) 129, 3770-3780 doi:10.1242/jcs.189332

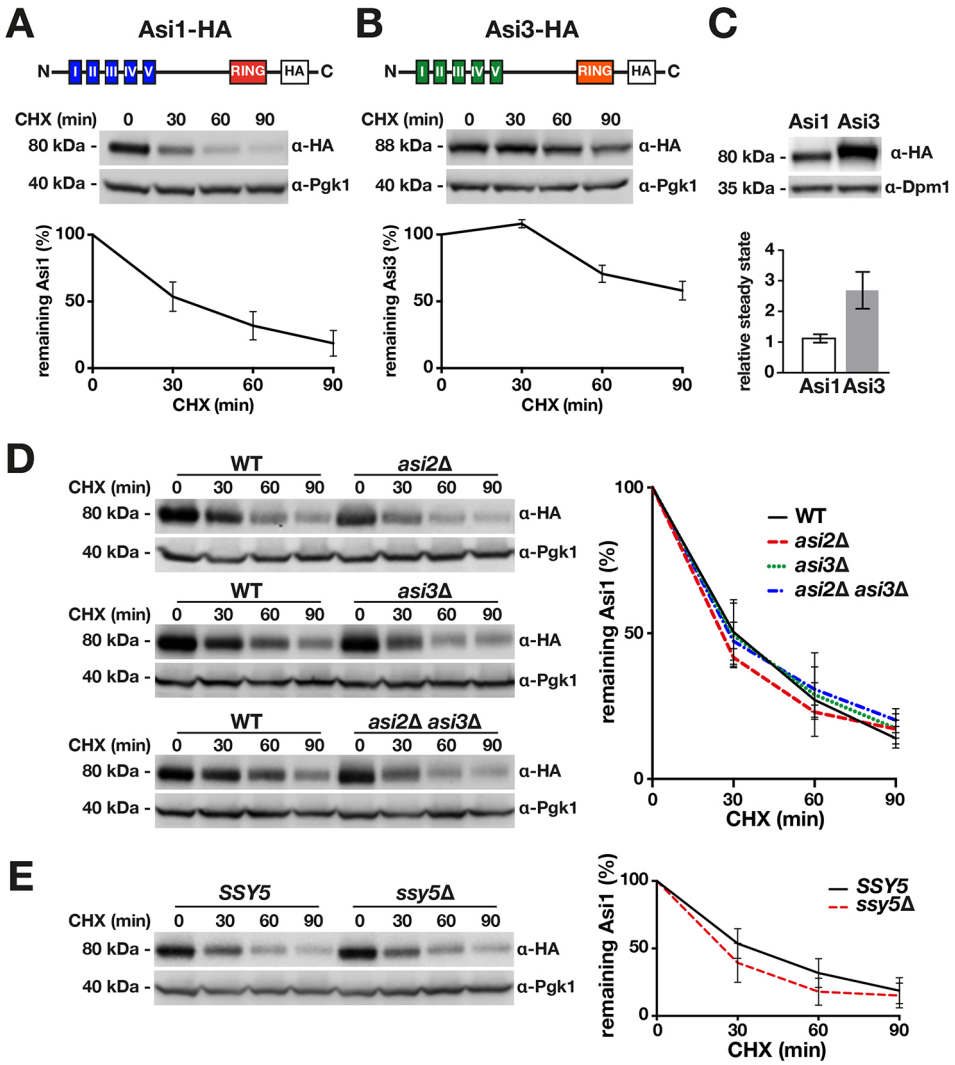

Fig. 1. Asi1 exhibits rapid turnover in a manner that is independent of Asi1–Asi3 E3 ubiquitin ligase and the SPS sensor. The stability of Asi1 (A) and Asi3 (B) was assessed by performing cycloheximide (CHX) chase. Top panels, schematic diagrams of Asi1–3HA (note the Asi1–6HA construct has similar a structure and placement of the HA tags) and Asi3–6HA; the positions of the five membrane-spanning segments (I–V), N-terminal RING finger domains and HA tags are depicted. Middle panels, CHX chase of Asi1–3HA (pPL1141) in *asi1*Δ (PLY1314), half-life=30 min; CHX chase of chromosomal Asi3–6HA in PLY1581, half-life >90 min. Extracts from cells harvested at the indicated times after CHX addition were resolved by SDS-PAGE, and the levels of Asi1 and Asi3 were assessed by immunoblotting using antibodies against HA (α-HA). The levels of Pgk1 (α-Pgk1) were used to control loading. Lower panels, the intensities of immunoreactive bands were quantified, and the average values from three independent experiments (*n*=3) were plotted as the percentage of Asi1 and Asi3 remaining after CHX addition; error bars represent s.d. (C) Relative steady-state protein levels of chromosome-encoded Asi1–6HA (PLY1811; taken as 1) and Asi3–6HA (PLY1581; ≈2.7× that of Asi1) (*n*=3; *P*=0.04). The levels of Dpm1 (α-Dpm1) were used to control loading. (D) CHX experiments of Asi1–3HA (pPL1141) in *asi1*Δ strains PLY1314 (WT, wild type), PLY1343 (*asi2*Δ), PLY1321 (*asi3*Δ) and PLY1346 (*asi2*Δ *asi3*Δ); half-lives were 30, 25, 30 and 25 min, respectively. *P*-values (60 min) WT compared to *asi2*Δ, 0.36; WT compared to *asi3*Δ, 0.85; WT compared to *asi2*Δ *asi3*Δ, 0.54. (E) Asi1 stability in strains that lacked the SPS-sensor component Ssy5. CHX chase of Asi1–3HA (pPL1141) in *SSY5* (PLY1314) and *ssy5*Δ (PLY1630) strains. Pgk1 was used as loading control. Average values and standard deviation (*n*=3) are plotted; the half-life of Asi1 in both strains ≈30 min, *P*-value (60 min) 0.14. *P*-values were calculated using two-tailed *t*-test, type 3.

2006). We addressed whether the rapid turnover of Asi1 is the consequence of a degradative pathway operating inside the nucleus. The stability of Asi1 was assessed in strains carrying the temperature sensitive *sts1-2* mutation. Sts1 interacts with the nuclear importin Srp1 to mediate the transport of inactive precursors of the proteasomal complexes into the nucleus. Consistently, Sts1 is required for proper assembly of nucleus-localized proteasomes (Chen et al., 2011; Romero-Perez et al., 2007). In *sts1-2* mutant cells shifted to the restrictive temperature, proteasomal activity in the nucleus gradually becomes depleted, resulting in the stabilization of nuclear substrates and the increased turnover of cytosolic substrates (Chen et al., 2011). Asi1 exhibited enhanced stability in an *sts1-2* mutant incubated at the non-permissive temperature (Fig. 2D). The results indicate that the bulk of Asi1 is degraded by proteasomes within the nucleus.

Asi1 turnover is Ubc7 dependent

To identify UPS components participating in the targeting of Asi1 for degradation, we examined the involvement of the E2 ubiquitin-conjugating enzymes Ubc6 and Ubc7. The stability of Asi1 was slightly enhanced in *ubc6*Δ cells and clearly enhanced in *ubc7*Δ cells (Fig. 3A). An additive effect on Asi1 stability was observed in *ubc6*Δ *ubc7*Δ double-mutant cells, consistent with a partial functional overlap. The involvement of Ubc6 and Ubc7 in the turnover of Asi1 is reflected by the enhanced steady-state levels of Asi1 in both *ubc6*Δ and *ubc7*Δ mutants (Fig. 3B). The deletion of

Journal of Cell Science (2016) 129, 3770-3780 doi:10.1242/jcs.189332

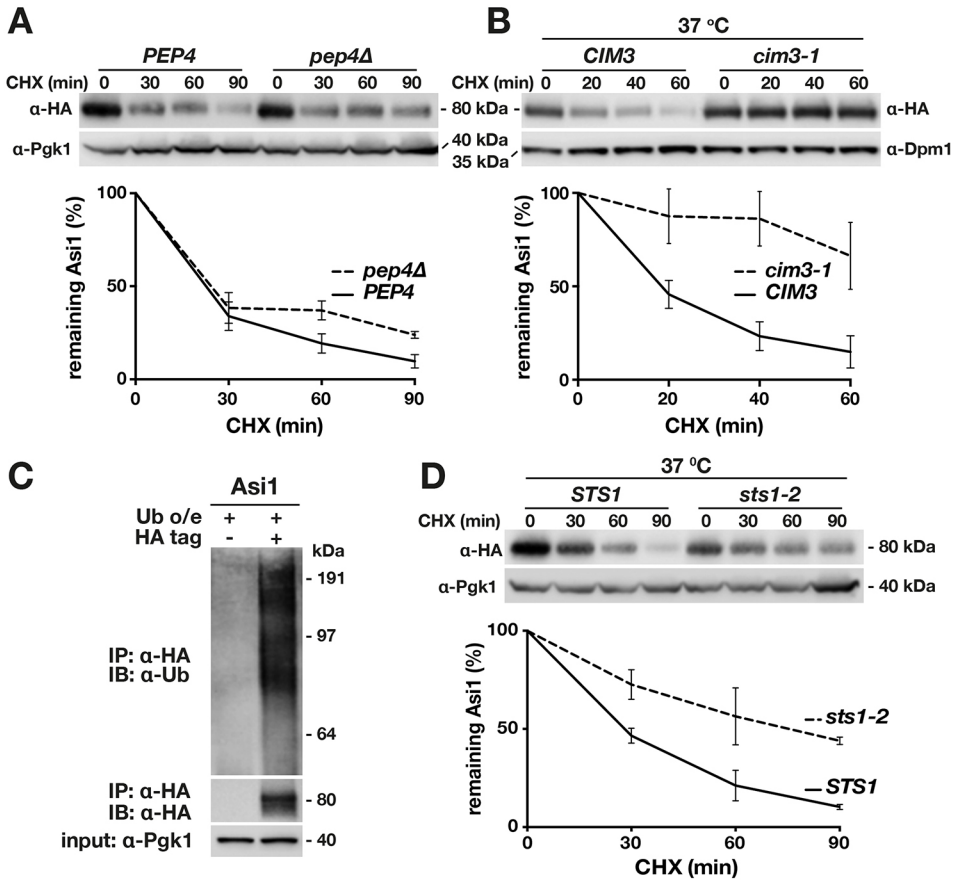

Fig. 2. Asi1 turnover is mediated by the ubiquitin proteasome system in the nucleus. (A) Asi1 is degraded independently of the major vacuolar peptidase Pep4. CHX chase of Asi1–3HA (pPL1141) in *PEP4* (PLY1327) and *pep4*Δ (YAZ101) strains. The graph plots the percentage of Asi1 remaining after CHX addition. Average values and s.d. (n=3) are plotted; half-life ≈25 min in both strains, P-value (60 min) 0.01. (B) Asi1 turnover is proteasome dependent. CHX chase of Asi1–3HA (pPL1141) in *CIM3* (CAY220) and temperature-sensitive *cim3-1* (PLY1348) strains. Cells were grown at 25°C (permissive temperature) and shifted to 37°C (non-permissive temperature) for 45 min before CHX addition. Extracts were prepared and immunoblotted for HA and Dpm1. The levels of Dpm1 were used to control loading. The graph represents the percentage of Asi1 remaining after CHX addition. Average values and s.d. (n=3) are plotted; half-life in *CIM3* ≈20 min and in *cim3-1* >60 min, P-value (40 min) 0.01. P-values were calculated using two-tailed t-test, type 3. (C) Asi1 is polyubiquitylated. Immunoprecipitation (IP:α-HA) of extracts prepared from PLY1314 (*asi1*Δ) carrying pPL1307 (P_{CUP1}-*6HIS-UBI*; Ub o/e) and pPL1136 (*ASI1-3HA*; HA-tag) or pAZ013 (*ASI1*, non-tagged control). o/e, overexpression. Immunoblot (IB) analysis was performed using anti-ubiquitin (IB:α-Ub) and anti-HA (IB:α-HA) antibodies. A portion (2%) of extract was immunoblotted for Pgk1 (input:α-Pgk1). (D) Asi1 is degraded by proteasomes in the nucleus. The stability of Asi1 in *STS1* (NA10) and *sts1-2* (NA25) strains expressing Asi1–3HA (pPL1141). Cells were grown at 25°C (permissive temperature) and shifted to 37°C (non-permissive temperature) for 3 h before CHX addition. Extracts from cells harvested at the indicated times were immunoblotted for HA and Pgk1. The graph represents the percentage of Asi1 remaining after CHX addition. Average values (n=3) and s.d. are plotted: half-life of Asi1 in *STS1* cells, 30 min and in *sts1-2*, 90 min; P-value (60 min) 0.03, calculated using two-tailed t-test, type 3. (See Fig. S1A for replicate immunoblots used to quantify the dependence of Asi1 stability on *STS1*.)

UBC7 did not affect *ASI1* mRNA expression (Fig. 3C), indicating that the increased level of Asi1 in *ubc7*Δ mutants is due to decreased protein turnover. The clear and distinct requirement for Ubc7 is consistent with its pronounced role in multiple protein quality control systems operating at the INM – e.g. the Asi1–Asi3-dependent degradation of soluble mislocalized transcription factors Stp1 and Stp2 (Khmelinskii et al., 2014), and the Doa10-dependent degradation of MATα2 repressor (Deng and Hochstrasser, 2006) and Asi2 (Boban et al., 2014).

Asi1 turnover is independent of the characterized ERAD and INMAD E3 ubiquitin ligases

Consistent with Asi1 being a resident of the INM, the turnover of Asi1 proceeded independently of the ERAD E3 ubiquitin ligase Hrd1 (Fig. 4A, upper panel). The stability of Asi1 was slightly enhanced in *doa10*Δ (Fig. 4A, middle panel) and *hrd1*Δ *doa10*Δ cells (Fig. 4A, lower panel). To more rigorously test the involvement of Doa10, we constructed a quadruple-mutant strain that lacked *ASI1*, *ASI2*, *ASI3* and *DOA10*, and analyzed the turnover of Asi1 and Asi2. The data indicate that Asi1 degradation occurs rapidly and independently of functional Asi1–Asi3 and Doa10 E3 ubiquitin ligase complexes (Fig. 4B and D). By contrast, and consistent with our previous studies, Asi2 turnover is clearly dependent on Doa10 (Fig. 4C and E) (Boban et al., 2014). Taken together, these results demonstrate that the stability of Asi1 and Asi2 is governed by the action of different E3 ubiquitin ligases, and that the E3 ubiquitin ligase controlling Asi1 turnover is not one of the two characterized INMAD ligases. Consequently, additional E3 ubiquitin ligases must operate in the INM to target Asi1 for degradation.

Genetic screening identifies Ubc7, Cue1, Cdc48 and Ubx1 as being required for Asi1 turnover

To identify additional INMAD components that contribute to the rapid turnover of Asi1, we assessed the stability of Asi1 in a panel of 86 strains (Table 1, generously provided by Mark Hochstrasser, Yale University) carrying loss-of-function mutations in genes

Journal of Cell Science (2016) 129, 3770-3780 doi:10.1242/jcs.189332

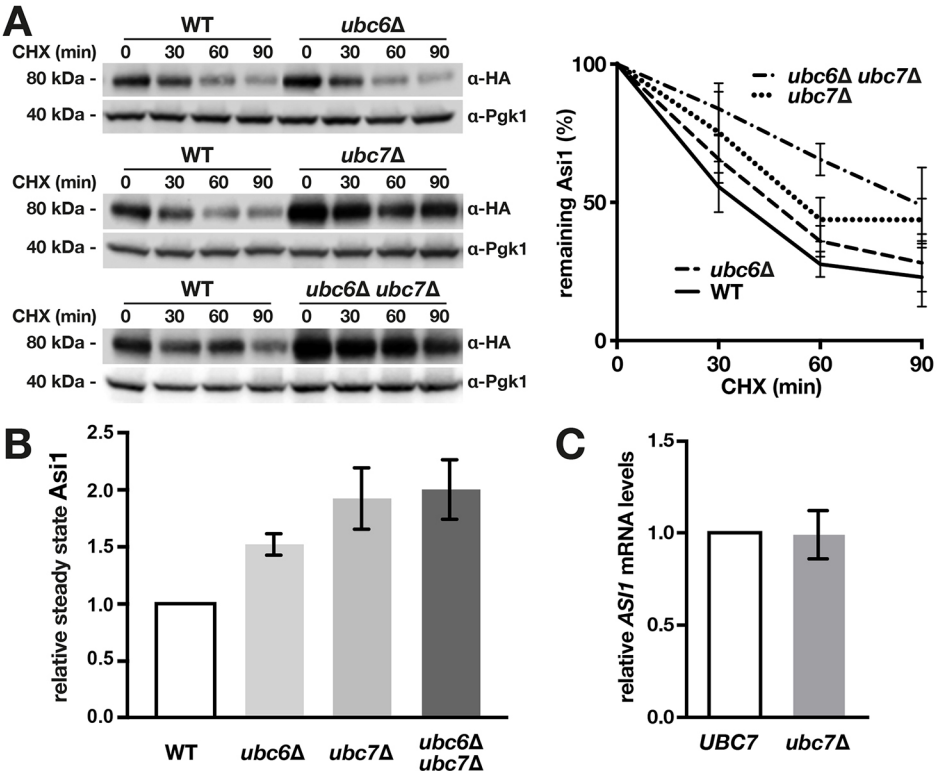

Fig. 3. Asi1 turnover is largely Ubc7 dependent. (A) CHX chase of Asi1–3HA (pPL1141) in wild-type (WT; MBY150), *ubc6*Δ (MBY151), *ubc7*Δ (MBY152) and *ubc6*Δ *ubc7*Δ (MBY153) cells. The graph represents the percentage of Asi1 remaining after CHX addition. Average values and s.d. (n=3) are plotted: half-life in WT 30 min, *ubc6*Δ 45 min, *ubc7*Δ 55 min, *ubc6*Δ *ubc7*Δ 90 min; P-values (60 min): WT compared to *ubc6*Δ, 0.04; WT compared to *ubc7*Δ, 0.03; WT compared to *ubc6*Δ *ubc7*Δ, 0.001. (B) Relative Asi1 steady-state protein levels in *ubc6*Δ (MBY151), *ubc7*Δ (MBY152) and *ubc6*Δ *ubc7*Δ (MBY153) cells normalized to those in WT (MBY150; taken as 1). (C) Relative *ASI1* mRNA levels were determined using qRT-PCR in *UBC7* (MBY150) and *ubc7*Δ (MBY152) strains expressing Asi1–3HA (pPL1141). Data represent relative *ASI1* mRNA amounts (arbitrary units, AU) normalized to those of *UBC7*. Average values and s.d. for three independent samples are shown.

encoding known components that operate in multiple degradation pathways. A plasmid carrying Asi1–3HA (pPL1141) was introduced into each strain, and the stability of Asi1 was assessed 60 min after CHX was added. The mutant collection included 39 E3 ubiquitin ligases, including RING, HECT and PHD proteins, and F-box proteins. Compared to wild-type control strains, with the exception of Doa10, none of these candidates showed any significant effect on turnover of Asi1; consistent with the data shown in Fig. 4A, the *doa10*Δ mutant reproducibly exhibited slightly higher levels of Asi1 remaining at the 60 min time point. Notably, Asi1 turnover was independent of San1, an important non-membrane E3 ubiquitin ligase in the nucleus (Rosenbaum et al., 2011). Although the lack of San1 involvement was expected – i.e. Asi1 does not fit the profile of San1 substrates – we examined Asi1 turnover in *asi2*Δ *san1*Δ *hrd1*Δ *doa10*Δ and *asi1*Δ *san1*Δ *hrd1*Δ *doa10*Δ quadruple-mutant strains. Asi1 turnover occurred unimpeded (data not shown), providing independent confirmation that San1 does not recognize Asi1 as a ubiquitylation substrate.

Additionally, all of the 13 Ubc proteins were tested for their influence on Asi1 turnover, including a *ubc4*Δ *ubc5*Δ double-mutant strain. The experiments confirmed the strong involvement of Ubc7 (Fig. 5A), again providing independent confirmation of results from our more-directed approach (Fig. 3). Moreover, 35 accessory proteins of the UPS were examined. Cue1 was found to participate in the degradation of Asi1 (Fig. 5A). Cue1 is an integral protein that tethers Ubc7 to the membranes, activates the E2 ubiquitin-conjugating enzyme and prevents its degradation (Bazirgan and Hampton, 2008; Biederer et al., 1997; Kostova et al., 2009). Also, consistent with Asi1 being a proteasomal substrate (Fig. 2B), Asi1 is significantly stabilized in the strain lacking *RPN4*. *RPN4* encodes a transcription factor that regulates the expression of proteasome subunit genes (Mannhaupt et al., 1999). Rpn4 function is well characterized and known to be required to maintain normal levels of intracellular proteolysis (Mannhaupt et al., 1999; Xie and Varshavsky, 2001).

Of the remaining mutants tested, we found that inactivation of the AAA ATPase Cdc48 and Ubx1(Shp1) strongly affected the stability of Asi1 (Fig. 5B and C, respectively). Cdc48 acts as a key regulator of the ubiquitin–proteasome pathway, interacting with a large number of interaction partners and co-factors that regulate its subcellular localization and substrate specificity (Buchberger, 2013; Meyer et al., 2012). The function of Ubx1 in yeast is not well established; however, Ubx2 has been implicated as an adaptor component of Cdc48 complexes involved in a variety of cellular processes (Bohm and Buchberger, 2013; Krick et al., 2010; Schuberth and Buchberger, 2005; Schuberth et al., 2004). The deletion of *UBX1* did not affect *ASI1* mRNA expression (Fig. 5C, right panel), indicating that the increased level of Asi1 in *ubx1*Δ mutants is due to decreased protein turnover. Our data demonstrate a new role for Cdc48 and Ubx1 as components of protein quality control pathway functioning at the INM.

DISCUSSION

The INM is the least-characterized membrane in eukaryotic cells, particularly with respect to the parameters affecting turnover of its integral membrane components (Boban and Foisner, 2016). To obtain mechanistic insight into the quality control systems operating in association with the INM, we have investigated the turnover of three native well-characterized and fully functional INM proteins as paradigmatic INMAD substrates – i.e. Asi1, Asi2 and Asi3 (Boban et al., 2006; Forsberg et al., 2001; Zargari et al., 2007). The Asi proteins exhibit distinct turnover rates – Asi1 $t_{1/2}\leq$30 min, Asi2 $t_{1/2}\approx$45 min and Asi3 $t_{1/2}>$90 min (Fig. 1, and see Boban et al., 2014). By examining the mechanisms that control Asi1 turnover, we have found that Asi1 is ubiquitylated in a unique quality control pathway associated with the INM (Figs 2, 3 and 5). Strikingly, Asi1 turnover occurs independently of the known INMAD pathways

Journal of Cell Science (2016) 129, 3770-3780 doi:10.1242/jcs.189332

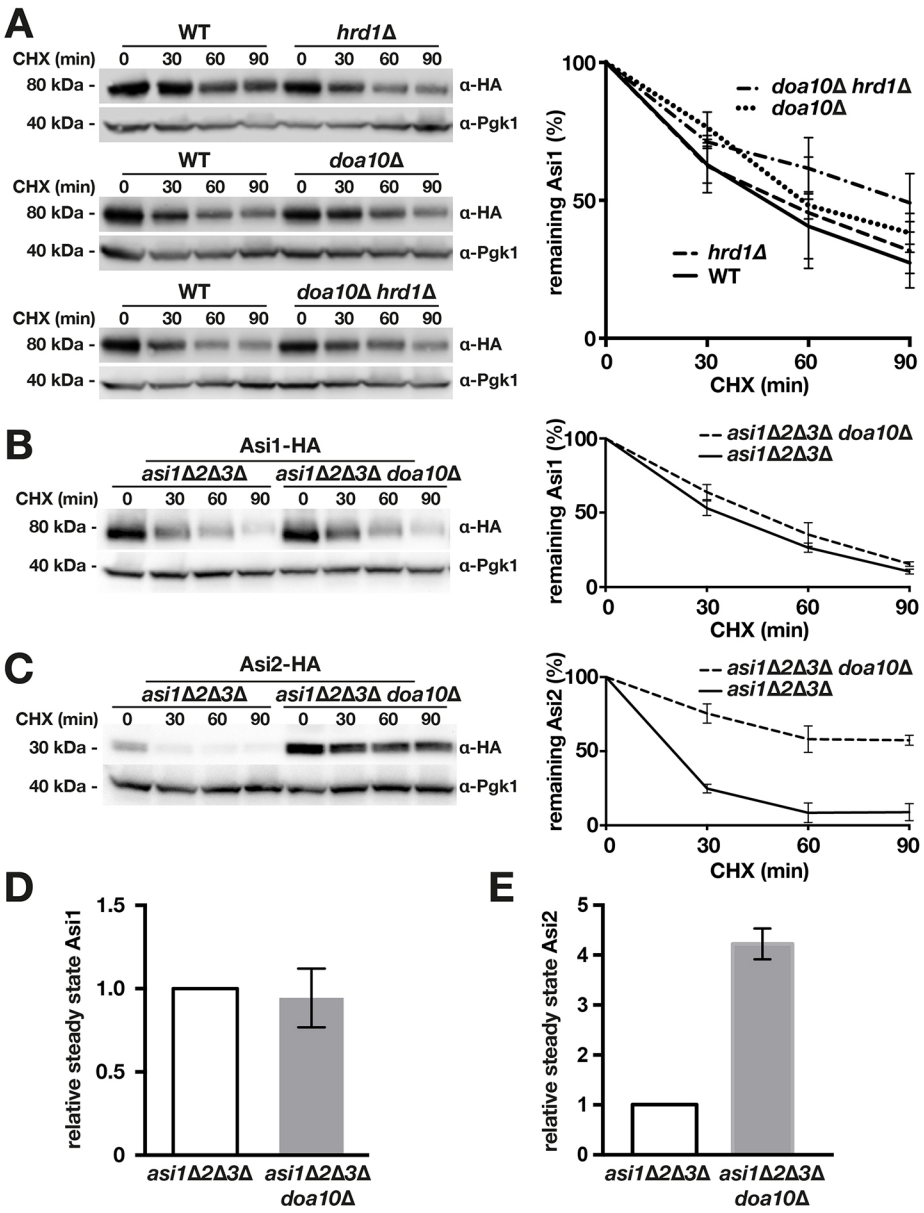

Fig. 4. Asi1 turnover occurs independently of the characterized Asi1–Asi3 and Doa10 INMAD E3 ligase complexes. (A) Asi1 turnover in *hrd1*Δ, *doa10*Δ and *doa10*Δ *hrd1*Δ mutant cells. CHX chase of Asi1–3HA (pPL1159) in wild-type (WT; MBY154), *hrd1*Δ (MBY155), *doa10*Δ (MBY156) and *doa10*Δ *hrd1*Δ (MBY157) strains. The graph represents the percentage of remaining Asi1 after CHX addition. Average values with s.d. (n=3) are plotted: half-life in WT 45 min, *hrd1*Δ 50 min, *doa10*Δ 60 min, and *doa10*Δ *hrd1*Δ 90 min; P-values (60 min) WT compared to *hrd1*Δ 0.74, WT compared to *doa10*Δ 0.38, and WT compared to *doa10*Δ *hrd1*Δ 0.09. P-values were calculated using two-tailed t-test, type 3. (See Fig. S1B for replicate immunoblots used to quantify the dependence of Asi1 stability on *HRD1*.) (B) Asi1 (pPL1141) and (C) Asi2 (pPL1142) turnover in *asi1*Δ*asi2*Δ*asi3*Δ (PLY1346; *asi1*Δ2Δ3Δ) and *asi1*Δ*asi2*Δ*asi3*Δ *doa10*Δ (PLY1947; *asi1*Δ2Δ3Δ *doa10*Δ). The graphs represent the percentage of remaining Asi1 and Asi2 at the indicated times after CHX addition; average values with s.d. (n=3) are plotted; Asi1 half-life in *asi1*Δ2Δ3Δ, 30 min; and *asi1*Δ2Δ3Δ *doa10*Δ, 45 min. Asi2 half-life in *asi1*Δ2Δ3Δ, 20 min and *asi1*Δ2Δ3Δ *doa10*Δ, >90 min; Asi1 P-values (60 min) *asi1*Δ2Δ3Δ compared to *asi1*Δ2Δ3Δ *doa10*Δ, 0.15; and Asi2, P-values (60 min) *asi1*Δ2Δ3Δ compared to *asi1*Δ2Δ3Δ *doa10*Δ, 0.002. P-values were calculated using two-tailed t-test, type 3. Relative steady-state protein levels of Asi1 (D) and Asi2 (E) in *asi1*Δ2Δ3Δ (PLY1346; taken as 1) and *asi1*Δ2Δ3Δ *doa10*Δ (PLY1947) cells. Data are mean±s.d.

(Figs 1 and 4 and Table 1), indicating that the INM possesses additional quality control systems (Fig. 6).

The clear difference in rates of Asi1 and Asi3 turnover and the finding that their turnover occurs largely independent of each other are noteworthy. These proteins are homologous, share similar structural features – including a C-terminal RING domain – co-purify and function together as subunits of the Asi1–Asi3 E3 ubiquitin ligase complex (Foresti et al., 2014; Khmelinskii et al., 2014; Zargari et al., 2007). Thus, although the Asi1–Asi3 E3 ubiquitin ligase operates together with the E2 ubiquitin-conjugating enzymes Ubc6 and Ubc7, and plays an essential role in clearing the nuclear compartment of mislocalized soluble and integral membrane proteins (Khmelinskii et al., 2014), this heterodimeric E3 ubiquitin ligase complex does not autoregulate the stability of its individual subunits. Our finding that the steady-state levels of Asi1 are significantly lower than those of Asi3 (Fig. 1C) suggests that the levels of Asi1 are limiting in the formation of the catalytically active Asi1–Asi3 E3 ubiquitin ligase complexes.

RING-deficient mutant forms of Asi1 that lack the ability to bind to Zn^{2+} are inactive. The *asi1-21HA* and *asi1-22HA* alleles, encoding mutant proteins with two and four of the Zn^{2+}-coordinating cysteine residues replaced with serine, respectively, precisely phenocopy the *asi1*Δ phenotype (Boban et al., 2006). Thus, an intact RING domain of Asi1 is an essential feature of the Asi1–Asi3 E3 ubiquitin ligase. We examined the turnover of the RING-mutant proteins and found that both are rapidly degraded in an *asi1*Δ mutant. Moreover, in control experiments, we found that their degradation occurred independently of Ubc7 (data not shown). Thus, the quality control pathway that controls the stability of the RING-deficient mutant proteins does not regulate the turnover of native and functional Asi1. Consequently, although consistent with our conclusion that Asi1 does not autoubiquitylate, the data regarding the turnover of the RING-mutant forms of Asi1 are difficult to properly interpret and unlikely to be relevant to furthering our understanding regarding the turnover of native Asi1.

In an effort to identify factors participating in native Asi1 turnover, we screened a collection of 86 mutant strains carrying defects in components of known protein degradation systems. This screen identified Ubc7, Cue1, Cdc48 and Ubx1 as being

Journal of Cell Science (2016) 129, 3770-3780 doi:10.1242/jcs.189332

Table 1. Genetic analysis of Asi1 stability

	E3 ligases								
	RING						Adaptor, accessory and ubiquitin-related proteins		
E2 UBC	SPRF		SCF	SUMO	HECT	PHD			
UBC1	*BRE1*	*RAD5*	*DIA2*	*HEX3*	*RSP5*	*ASR1*	***cdc48-3***	*HAL5*	***UBX1***
UBC2/RAD6	*DMA1*	*RAD18*	*GRR1*	*NFI1*	*TOM1*	*BYE1*	*cdc53-1*	*HUL4 (E4)*	*UBX2*
UBC3/cdc34-1	*DMA2*	*RKR1*	*UFO1*	*RIS1*		*CTI6*	***CUE1***[1]	*HUL5 (E4)*	*UBX3*
UBC4	***DOA10***[1]	*RMD5*		*SIZ1*		*IOC2*	*CUL3*	*PEP3*	*UBX4*
UBC5	*HRD1*	*SAN1*		*SLX8*		*NTO1*	*CUL8*	*PHO23*	*UBX5*
UBC6	*MAG2*	*SNT2*				*SPP1*	*DOA4*	*PRE9*	*UBX6*
UBC7[1]	*NOT4*	*TUL1*				*SET3*	*ECM3*	*RAD16*	*UBX7*
UBC8	*PEP5*	*UBR1*				*YNG1*	*FAP1*	*RCO1*	*UFD2 (E4)*
UBC9 (SUMO)	*PEX2*	*UBR2*					*FAR1*	***RPN4***[1]	*UFD3*
UBC10/PEX4	*PEX10*	*UFD4*					*FKS1*	*SET4*	*VPS8*
UBC11	*PIB1*						*GCN2*	*skp1-11*	
UBC12							*GIR2*	*STE5*	
UBC13							*GIS2*		

[1]Pronounced stability of Asi1 in strains carrying inactivating mutations (bold) compared to wild type; CHX chase at *t*=60 min.

required for Asi1 turnover but failed to identify a primary E3 ubiquitin ligase (Table 1, Fig. 5). This negative result could be the consequence of the involvement of an essential ligase or redundancy – perhaps multiple ligases contribute to regulating Asi1 stability. Interestingly, the two previously identified INMAD quality control systems and the new system we have shown to exist in this work share common components – i.e. the E2 ubiquitin-conjugating enzyme Ubc7 and its co-factor Cue1. Ubc7 has

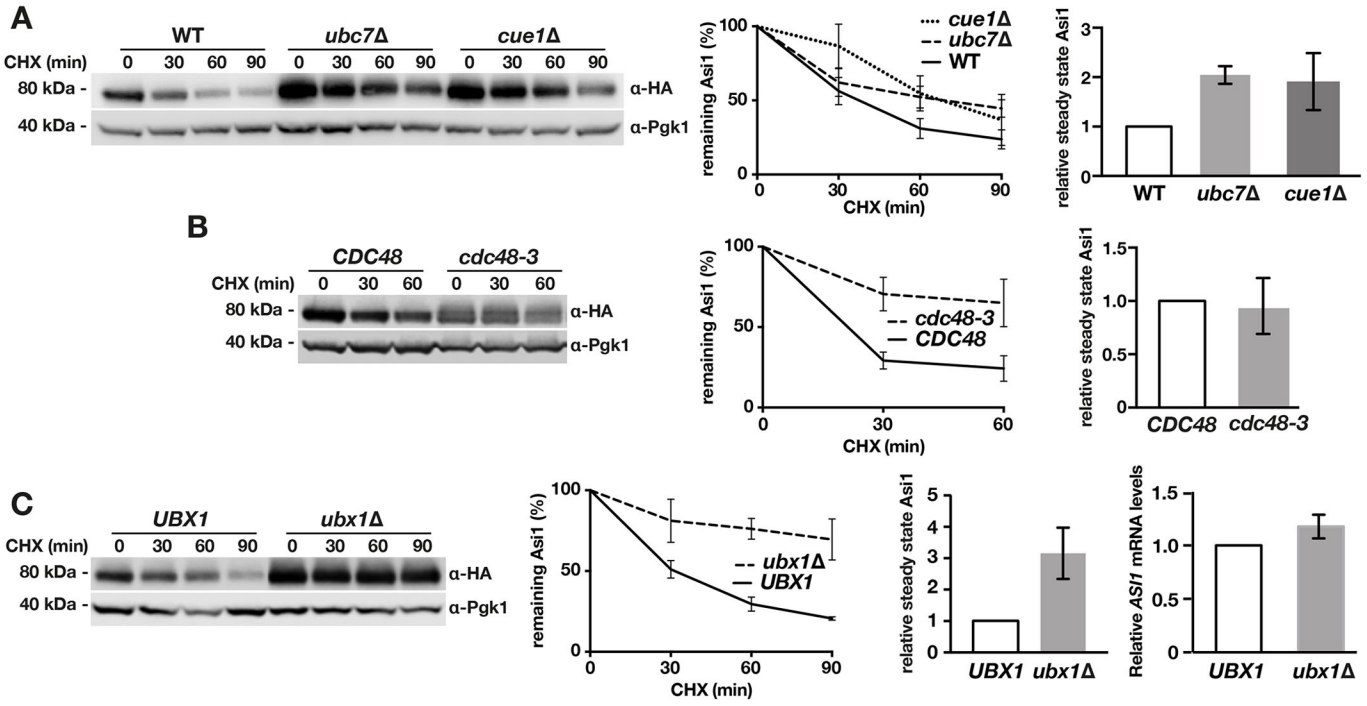

Fig. 5. Asi1 turnover is impaired in strains that lack Cue1, Cdc48 and Ubx1. (A) Asi1 turnover is impaired in *ubc7*Δ and *cue1*Δ mutants. CHX chase of Asi1–3HA (pPL1141) in wild-type (WT; BY4741), *ubc7*Δ (BY4741$_{ubc7\Delta}$) and *cue1*Δ (BY4741$_{cue1\Delta}$) cells (left panels). The percentage of Asi1 remaining after CHX addition is plotted as average values with s.d. (*n*=3): half-life in WT 30 min; *ubc7*Δ, 60 min; and *cue1*Δ, 60 min; *P*-values (60 min) WT compared to *ubc7*Δ, 0.05; WT compared to *cue1*Δ, 0.05 (middle panel). The relative steady-state protein levels of Asi1 in WT (BY4741; taken as 1), *ubc7*Δ (BY4741$_{ubc7\Delta}$) and *cue1*Δ (BY4741$_{cue1\Delta}$) cells are plotted (*n*=3; right panel). (B) Asi1 turnover is impaired in *cdc48-3* temperature-sensitive cells. CHX chase of Asi1–3HA (pPL1141) in *CDC48* (MHY1562) and *cdc48-3* (MHY3512) cells (left panels). Cultures were grown at 25°C (permissive temperature) and shifted to 37°C (non-permissive temperature) 1 h before CHX addition. The percentage of Asi1 remaining after CHX addition is plotted as average values with s.d. (*n*=3): half-life in *CDC48*, 20 min; and *cdc48-3*, >60 min; *P*-value (60 min), 0.02 (middle panel). The relative steady-state protein levels of Asi1 in *CDC48* (MHY1562; taken as 1) and *cdc48-3* (MHY3512) cells are plotted (*n*=3; right panel). (See Fig. S1C for replicate immunoblots used to quantify the dependence of Asi1 stability on *CDC48*.) (C) Asi1 turnover is impaired in *ubx1*Δ mutant cells. CHX chase of Asi1–3HA (pPL1141) in *UBX1* (BY4741) and *ubx1*Δ (BY4741$_{ubx1\Delta}$) cells (left panels). The percentage of Asi1 remaining after CHX addition is plotted as the average value with s.d. (*n*=3); half-life in *UBX1*, 30 min; and *ubx1*Δ, >90 min; *P*-value (60 min), 0.03. *P*-values were calculated using two-tailed *t*-test, type 3 (left middle panel). The relative steady-state protein levels of Asi1 in *UBX1* (BY4741; taken as 1) and *ubx1*Δ (BY4741$_{ubx1\Delta}$) cells are plotted (second panel from right). The relative *ASI1* mRNA levels in *UBX1* (BY4741; taken as 1) and *ubx1*Δ (BY4741$_{ubx1\Delta}$) strains expressing Asi1–3HA (pPL1141) (right panel). Data represent relative *ASI1* mRNA amounts; average values and s.d. (*n*=3) are shown. (See Fig. S1D for replicate immunoblots used to quantify the dependence of Asi1 stability on *UBX1*.)

Journal of Cell Science (2016) 129, 3770-3780 doi:10.1242/jcs.189332

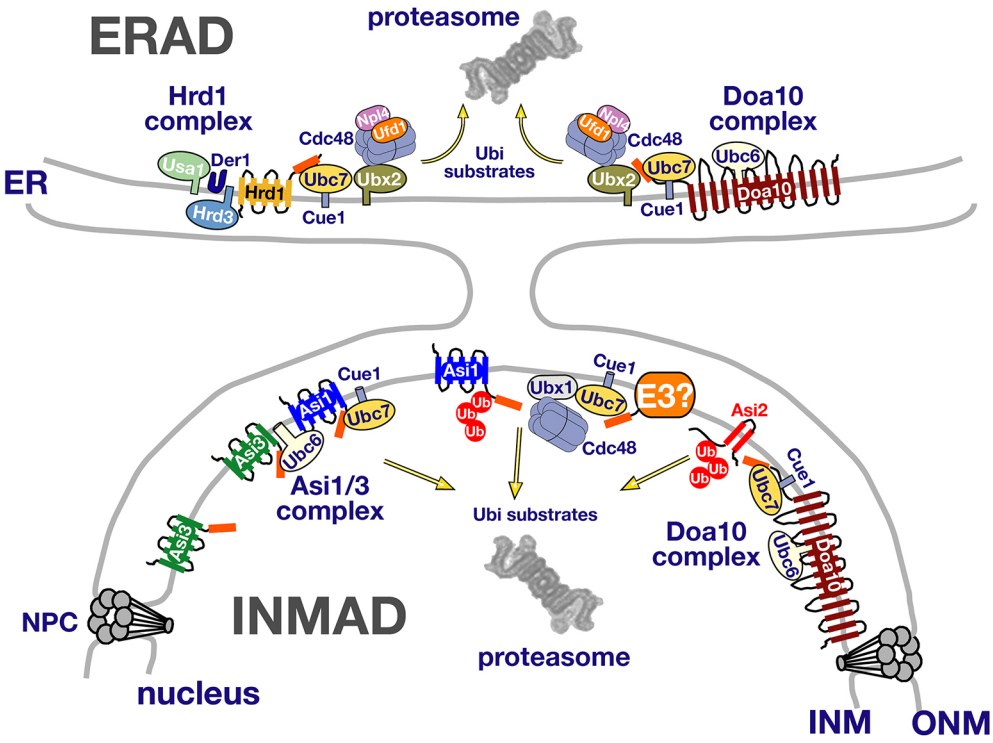

Fig. 6. Schematic diagram of known ERAD and INMAD pathways. The two major ERAD E3 ubiquitin ligase complexes, Hrd1 and Doa10, are depicted in the membrane of the ER (Carvalho et al., 2006; Denic et al., 2006; Hiller et al., 1996; Sommer and Jentsch, 1993; Werner et al., 1996). The ERAD complexes target substrates for degradation by proteasomes located in the cytoplasm. The two characterized INMAD E3 ubiquitin ligase complexes Asi1–Asi3 (Asi1/3 complex) and Doa10 are depicted in the INM. The INMAD complexes target substrates for degradation by proteasomes located in the nucleus. The results presented here indicate that Asi1 turnover is mediated by the E2 ubiquitin-conjugating enzyme Ubc7, and ubiquitylation is dependent on one, or more, as yet to be identified E3 ubiquitin ligase(s) (E3?). By contrast, Asi2 turnover primarily occurs in a Doa10 INMAD complex-dependent manner. The degradation of Asi1 requires dislocation from the INM, a process mediated by the $Cdc48^{Ubx1}$ complex. Ubi, ubiquitylation.

multiple roles in INM protein quality control. Together with the Asi1–Asi3 E3 ubiquitin ligase complex, it mediates degradation of the soluble transcription factors Stp1 and Stp2 when these factors ectopically enter the nucleus (Khmelinskii et al., 2014). Also, Ubc7 works with Doa10 to target transcription factor Matα2 (Chen et al., 1993; Deng and Hochstrasser, 2006) and Asi2 (Boban et al., 2014) for degradation.

The AAA ATPase Cdc48 participates in distinct cellular processes, acting as a key regulator of the ubiquitin–proteasome pathway (Buchberger, 2013; Meyer et al., 2012). Ubiquitylated membrane proteins that have been tagged for degradation by proteasomes must be extracted, or dislocated, from the membrane. Although proteasomes could contribute to this process, Cdc48 is thought to be the most important facilitator of the dislocation of ubiquitylated substrate proteins. Cdc48 is directed to different degradative pathways within the cell, where its activity is regulated and is dependent on the action of adaptor proteins – i.e. UBX-domain-containing proteins (Buchberger et al., 2015; Neuber et al., 2005; Schuberth and Buchberger, 2008). In yeast, there are seven UBX proteins. Ubx2, the best-characterized UBX protein, resides in the ER where it is thought to recognize polyubiquitylated substrates exposed on the cytosolic face of the ER and to be in complex with Cdc48 ($Cdc48^{Ubx2}$), facilitating dislocation of the ubiquitylated proteins from the ER (Kolawa et al., 2013; Neuber et al., 2005; Schuberth and Buchberger, 2005). At the ER, Ufd1 and Npl4 are associated with $Cdc48^{Ubx2}$ (Jentsch and Rumpf, 2007). We found that Ubx1, the least-characterized UBX protein, is stringently required for Asi1 turnover. Analogous to Ubx2, Ubx1 could function by recruiting Cdc48 to the INM, forming a complex that facilitates the membrane dislocation of ubiquitylated Asi1 and potentially other ubiquitylated INM proteins, a requisite for their degradation by nuclear proteasomes.

Ubx1 has been implicated in regulating the activity of the protein phosphatase 1 (Glc7) during cell cycle progression, participating in the ubiquitin-dependent proteasomal degradation of ubiquitylated phosphorylated β-galactosidase and in Atg8-dependent piecemeal microautophagy of the nucleus (PMN) (Bohm and Buchberger, 2013; Krick et al., 2010; Schuberth et al., 2004). PMN is a process whereby parts of the nucleus are degraded by the vacuole (Pan et al., 2000; Roberts et al., 2003). Under nitrogen starvation, the yeast INM protein Src1 and ER and ONM protein Hmg1 are directed for vacuolar degradation through autophagic sequestration into double-membraned vesicles derived from the nuclear envelope (Mochida et al., 2015). Thus, perhaps under nutrient limitation or other cell stress, Asi1 is targeted through PMN to the vacuole in a Ubx1- and Atg8-dependent manner. However, in the absence of nutrient stress, as in the experimental conditions used in our studies, Ubx1 is likely to function together with Cdc48 to facilitate membrane dislocation of ubiquitylated substrates, as described in the preceding paragraph.

Based on cumulating information, the Asi1–Asi3 and Doa10 E3 ubiquitin ligase complexes clearly function as non-redundant quality control pathways within the INM. This notion is supported by a number of observations. The spectrum of proteins stabilized by mutations inactivating Asi1 and Asi3 exhibit extensive overlap (Khmelinskii et al., 2014), a finding consistent with the obligate functional interdependence in the Asi1–Asi3 E3 ubiquitin ligase complex. By contrast, there is little overlap with proteins that are stabilized by inactivating Doa10. Consequently, these E3 ubiquitin ligases have distinct substrate specificities. Also, there are no observable additive effects by combining *asi1*Δ with *doa10*Δ *hrd1*Δ on the stability of proteins exhibiting Asi1–Asi3 dependence; substrate proteins exhibit indistinguishable rates of turnover in *asi1*Δ and in the triple mutant *asi1*Δ *hrd1*Δ *doa10*Δ (Khmelinskii et al., 2014). Finally, null alleles of *DOA10* do not induce constitutive SPS-sensor-regulated gene expression; apparently, Doa10 does not recognize the N-terminal nuclear degrons of Stp1 and Stp2 (Khmelinskii et al., 2014; Omnus and Ljungdahl, 2014). Thus, the characterized INMAD pathways are clearly separate from each other and also distinct from the well-characterized ERAD

Journal of Cell Science (2016) 129, 3770-3780 doi:10.1242/jcs.189332

pathways defined by the Hrd1 and Doa10 E3 ubiquitin ligases that target ubiquitylated proteins for degradation by proteasomes in the cytoplasm (Fig. 6).

The multiple INMAD pathways controlling the turnover of INM proteins target their ubiquitylated substrates to nucleus-localized proteasomes (Fig. 3, and see Boban et al., 2014). Proteasomes account for 80–90% of protein turnover in rapidly growing yeast cells (Enenkel, 2014). The nucleus is enriched with proteasomes, indicating that nuclear protein quality control is important in proliferating yeast cells as it secures DNA stability and repair, DNA replication, chromosome segregation, transcription and gene silencing (Chowdhury and Enenkel, 2015; Wojcik and DeMartino, 2003). In this context, cytosolic proteasomes are indispensable for yeast growth, whereas nuclear proteasomes are essential for viability (Tsuchiya et al., 2013). Additionally, there is growing evidence that diverse cytosolic proteins are translocated to the nucleus and are degraded by nuclear proteasomes through chaperone-dependent delivery and ubiquitylation by the nuclear E3 ubiquitin ligase San1 (Guerriero et al., 2013; Heck et al., 2010; Park et al., 2013; Prasad et al., 2010). Hence, the discovery that multiple INMAD pathways exist bolsters the notion that the nuclear compartment is well equipped as a major site for protein quality control.

Extremely little is known regarding the turnover of INM proteins. Thus, our findings that multiple quality control INMAD pathways exist represent new and important insights into the biology of eukaryotic cells. In contrast to metazoan cells, yeast cells exhibit closed mitosis, meaning that the nuclear envelope remains intact throughout the cell cycle (Anderson and Hetzer, 2008). Thus, the yeast INMAD pathways enable cells to maintain the integrity of the INM by removing genuine INM proteins that become damaged or aged and by eliminating proteins that mislocalize to the INM. Perhaps one of the most important implications of recent findings regarding the biological function of INMAD pathways is that many membrane proteins that primarily localize elsewhere slip past the barrier function of nuclear pore complexes and gain access to the INM (Foresti et al., 2014; Khmelinskii et al., 2014; Popken et al., 2015). These unexpected observations undoubtedly provide the biological requirement for multiple quality control systems associated with this important membrane. Apparently, INMAD pathways provide cells with solutions to the inherently difficult challenge of creating fail-safe targeting mechanisms to ensure the proper composition of the nuclear compartment. Although it is presently unclear whether similar INMAD quality control pathways exist outside of yeast, our findings will hopefully encourage others to pursue the possibility that functional INMAD pathways exist and operate analogously in other organisms. Clearly, safeguarding the integrity of the INM must be a crucial and common concern shared by most, if not all, eukaryotic cells. The importance of membrane-associated protein degradation mechanisms and the large diversity of integral membrane RING domain proteins in mammalian cells suggest that such research will lead to fruitful findings.

MATERIALS AND METHODS

Yeast growth media

Standard yeast growth media were used, including yeast-extract-peptone-dextrose (YPD) medium and ammonia-based synthetic complete dextrose (SC) and ammonia-based synthetic minimal dextrose (SD) medium, supplemented as required to enable the growth of auxotrophic strains, prepared as described previously (Andréasson and Ljungdahl, 2002). Antibiotic selections were made on solid YPD containing 200 mg/l G418 or 100 mg/l clonNAT.

Strains and plasmids

Saccharomyces cerevisiae strains used in this study (Table S1) are isogenic descendants of the S288c-derived strain AA255/PLY115, except for *sts1-2*, provided by Kiran Madura (Robert Wood Johnson Medical School, Rutgers University, NJ), and *cdc48-3* (W303-1B background) provided by Dr Mark Hochstrasser (Yale University, CT). The EUROSCARF deletion library used in our screen, and generously provided by Dr Hochstrasser, consists of BY4741-derived strains that are considered to be isogenic to the S288c genetic background. The temperature-sensitive strains *cdc34-1*, *cdc53-1* and *skp1-11* provided by Dr Bruno André (Université Libre de Bruxelles, Belgium) are isogenic descendants of the W303-1B and MT235 strain background. The plasmids used in this study are listed in Table S1. The sequences of mutagenic oligonucleotides and PCR primers for homologous recombination are available upon request.

Cycloheximide experiments and immunoblot analysis

Yeast strains were grown at 30°C, unless indicated otherwise, to OD_{600} of 0.8–1. CHX (Sigma-Aldrich) was added to cultures (final concentration of 100 µg/ml), and samples were harvested at indicated time points. Total protein extracts were prepared under denaturing conditions using NaOH and trichloroacetic acid, as described previously (Boban et al., 2014). The following antibodies were used for immunoblot analysis: horseradish peroxidase (HRP)-conjugated rat monoclonal anti-HA (3F10, 1:5000; Roche Applied Science), mouse monoclonal anti-Pgk1 (22C5, 1:5000; Molecular Probes), mouse monoclonal anti-Dpm1 (5C5, 1:1000; Molecular Probes) and HRP-conjugated goat anti-mouse (1:5000; Roche Applied Science) antibodies. Enhanced chemiluminescence (SuperSignal West Dura Extended Duration Substrate, Thermo Scientific) signals were detected using a BIO-RAD ChemiDoc XRS+ system and quantified with BIO-RAD image Lab 3.0 build 11. The sum of the signal intensity of Asi1 bands was normalized to the signal of the stable protein control Dpm1 or Pgk1. In each experiment, average values, s.d. and *P*-values based on three independent samples were calculated.

Ubiquitylation assay

Yeast lysates from strains expressing Asi1–3HA (pPL1136) or Asi1 (pAZ013) and carrying ubiquitin-overexpression plasmid pPL1307 (PCUP1-6HIS-UBI) were immunoprecipitated using anti-HA affinity matrix (rat monoclonal 3F10, Roche Applied Science), as described previously (Boban et al., 2014). Immunoblot analysis was performed using mouse monoclonal anti-ubiquitin (P4D1, 1:0000; Santa Cruz), HRP-conjugated rat monoclonal anti-HA (3F10, 1:5000; Roche Applied Science), mouse monoclonal anti-Pgk1 (22C5, 1:5000; Molecular Probes) and HRP-conjugated goat anti-mouse (1:5000; Roche Applied Science) antibodies.

RNA isolation and qRT-PCR

Exponentially growing cells in SC medium (≈10^7 cells) carrying pPL1141 (*ASI1-3HA*) were harvested by centrifugation. RNA was isolated using the RiboPure Yeast Kit (Ambion by Life Technologies) and treated with Turbo-DNase (Ambion by Life Technologies). One microgram of RNA was used for complementary DNA synthesis with oligo (dT)12-19 (Invitrogen by Life Technologies) using SuperScript III Reverse Transcriptase (Life Technologies). Quantitative reverse transcriptase PCR (qRT-PCR) reactions were prepared using Kapa SybrFast qPCR Master Mix (Kapa Biosystems). The absence of DNA contamination was confirmed using minus reverse transcriptase samples. The cDNA preparations were diluted 1:40, and 5 µl was used in a reaction volume of 20 µl. The levels of gene expression in three biological replicates were determined in three separate amplifications with triplicate technical replicates of each of the two genes analyzed using the comparative ΔC_T method (RotorGene 6000, Corbett Life Science). Relative levels of *ASI1* messenger RNA were normalized with respect to the levels of the invariant reference gene *TAF10*. The following primer pairs were used: ASI1-3HA fwd 5′-GGCCCTGCCGATGTTTTGCC-3′ and ASI1-3HA rev 5′-GGGACGTCATAGGGATAGCC-3′; TAF10 fwd 5′-A-TATTCCAGGATCAGGTCTTCCGTAGC-3′ and TAF10 rev 5′-CAACA-ACAACATCAACAGAATGAGAAGACTAC-3′.

Acknowledgements
Portions of the data have been discussed in the Ph.D. thesis of Marina Pantazopoulou (Protein Quality Control at the Inner Nuclear Membrane – The Asi complex in *Saccharomyces cerevisiae*, 2016, Stockholm University, Sweden). We thank Mark Hochstrasser, Bruno André and Kiran Madura for plasmids and yeast strains. Our Ljungdahl laboratory colleagues Antonio Martins, Andreas Ring and Kicki Ryman are gratefully acknowledged for contributions to the revision process.

Competing interests
The authors declare no competing or financial interests.

Author contributions
Conceptualization: M.P., M.B., P.O.L.; Methodology: M.P., M.B., P.O.L.; Formal analysis and investigation: M.P.; Writing – original draft preparation: M.P., P.O.L.; Writing – review and editing: M.P., M.B., R.F., P.O.L.; Visualization: M.P., P.O.L.; Supervision: R.F., P.O.L.; Project Administration: R.F., P.O.L.; Funding acquisition: M.B., R.F., P.O.L.

Funding
The authors acknowledge grant support from the Swedish Research Council (Vetenskapsrådet) [grant numbers VR-NT2011-5925 and VR-NT2015-04202 (P.O. L.)]; the Austrian Science Fund [FWF; grant number P23805-B20 (R.F.)]; and a European Molecular Biology Organization long-term fellowship (M.B.).

Supplementary information
Supplementary information available online at
http://jcs.biologists.org/lookup/doi/10.1242/jcs.189332.supplemental

References

Ammerer, G., Hunter, C. P., Rothman, J. H., Saari, G. C., Valls, L. A. and Stevens, T. H. (1986). *PEP4* gene of *Saccharomyces cerevisiae* encodes proteinase A, a vacuolar enzyme required for processing of vacuolar precursors. *Mol. Cell. Biol.* **6**, 2490-2499.
Anderson, D. J. and Hetzer, M. W. (2008). The life cycle of the metazoan nuclear envelope. *Curr. Opin. Cell Biol.* **20**, 386-392.
Andréasson, C. and Ljungdahl, P. O. (2002). Receptor-mediated endoproteolytic activation of two transcription factors in yeast. *Genes Dev.* **16**, 3158-3172.
Bays, N. W., Gardner, R. G., Seelig, L. P., Joazeiro, C. A. and Hampton, R. Y. (2001). Hrd1p/Der3p is a membrane-anchored ubiquitin ligase required for ER-associated degradation. *Nat. Cell Biol.* **3**, 24-29.
Bazirgan, O. A. and Hampton, R. Y. (2008). Cue1p is an activator of Ubc7p E2 activity in vitro and in vivo. *J. Biol. Chem.* **283**, 12797-12810.
Biederer, T., Volkwein, C. and Sommer, T. (1997). Role of Cue1p in ubiquitination and degradation at the ER surface. *Science* **278**, 1806-1809.
Boban, M. and Foisner, R. (2016). Degradation-mediated protein quality control at the inner nuclear membrane. *Nucleus* **7**, 41-49.
Boban, M., Zargari, A., Andréasson, C., Heessen, S., Thyberg, J. and Ljungdahl, P. O. (2006). Asi1 is an inner nuclear membrane protein that restricts promoter access of two latent transcription factors. *J. Cell Biol.* **173**, 695-707.
Boban, M., Pantazopoulou, M., Schick, A., Ljungdahl, P. O. and Foisner, R. (2014). A nuclear ubiquitin-proteasome pathway targets the inner nuclear membrane protein Asi2 for degradation. *J. Cell Sci.* **127**, 3603-3613.
Böhm, S. and Buchberger, A. (2013). The budding yeast Cdc48(Shp1) complex promotes cell cycle progression by positive regulation of protein phosphatase 1 (Glc7). *PLoS ONE* **8**, e56486.
Bryant, N. J. and Stevens, T. H. (1998). Vacuole biogenesis in *Saccharomyces cerevisiae*: protein transport pathways to the yeast vacuole. *Microbiol. Mol. Biol. Rev.* **62**, 230-247.
Buchberger, A. (2013). Roles of Cdc48 in regulated protein degradation in yeast. *Subcell. Biochem.* **66**, 195-222.
Buchberger, A., Schindelin, H. and Hänzelmann, P. (2015). Control of p97 function by cofactor binding. *FEBS Lett.* **589**, 2578-2589.
Carvalho, P., Goder, V. and Rapoport, T. A. (2006). Distinct ubiquitin-ligase complexes define convergent pathways for the degradation of ER proteins. *Cell* **126**, 361-373.
Chau, V., Tobias, J. W., Bachmair, A., Marriott, D., Ecker, D. J., Gonda, D. K. and Varshavsky, A. (1989). A multiubiquitin chain is confined to specific lysine in a targeted short-lived protein. *Science* **243**, 1576-1583.
Chen, P., Johnson, P., Sommer, T., Jentsch, S. and Hochstrasser, M. (1993). Multiple ubiquitin-conjugating enzymes participate in the in vivo degradation of the yeast MAT alpha 2 repressor. *Cell* **74**, 357-369.
Chen, L., Romero, L., Chuang, S.-M., Tournier, V., Joshi, K. K., Lee, J. A., Kovvali, G. and Madura, K. (2011). Sts1 plays a key role in targeting proteasomes to the nucleus. *J. Biol. Chem.* **286**, 3104-3118.
Chowdhury, M. and Enenkel, C. (2015). Intracellular dynamics of the ubiquitin-proteasome-system. *F1000Res.* **4**, 367.
Ciechanover, A. (2007). Intracellular protein degradation from a vague idea through the lysosome and the ubiquitin-proteasome system and on to human diseases and drug targeting: Nobel Lecture, December 8, 2004. *Ann. N. Y. Acad. Sci.* **1116**, 1-28.
Deng, M. and Hochstrasser, M. (2006). Spatially regulated ubiquitin ligation by an ER/nuclear membrane ligase. *Nature* **443**, 827-831.
Denic, V., Quan, E. M. and Weissman, J. S. (2006). A luminal surveillance complex that selects misfolded glycoproteins for ER-associated degradation. *Cell* **126**, 349-359.
Enenkel, C. (2014). Nuclear transport of yeast proteasomes. *Biomolecules* **4**, 940-955.
Foresti, O., Rodriguez-Vaello, V., Funaya, C. and Carvalho, P. (2014). Quality control of inner nuclear membrane proteins by the Asi complex. *Science* **346**, 751-755.
Forsberg, H., Hammar, M., Andréasson, C., Molinér, A. and Ljungdahl, P. O. (2001). Suppressors of *ssy1* and *ptr3* null mutations define novel amino acid sensor-independent genes in *Saccharomyces cerevisiae*. *Genetics* **158**, 973-988.
Friedlander, R., Jarosch, E., Urban, J., Volkwein, C. and Sommer, T. (2000). A regulatory link between ER-associated protein degradation and the unfolded-protein response. *Nat. Cell Biol.* **2**, 379-384.
Furth, N., Gertman, O., Shiber, A., Alfassy, O. S., Cohen, I., Rosenberg, M. M., Doron, N. K., Friedler, A. and Ravid, T. (2011). Exposure of bipartite hydrophobic signal triggers nuclear quality control of Ndc10 at the endoplasmic reticulum/nuclear envelope. *Mol. Biol. Cell* **22**, 4726-4739.
Ghislain, M., Udvardy, A. and Mann, C. (1993). *S.* cerevisiae 26S protease mutants arrest cell division in G2/metaphase. *Nature* **366**, 358-362.
Guerriero, C. J., Weiberth, K. F. and Brodsky, J. L. (2013). Hsp70 targets a cytoplasmic quality control substrate to the San1p ubiquitin ligase. *J. Biol. Chem.* **288**, 18506-18520.
Heck, J. W., Cheung, S. K. and Hampton, R. Y. (2010). Cytoplasmic protein quality control degradation mediated by parallel actions of the E3 ubiquitin ligases Ubr1 and San1. *Proc. Natl. Acad. Sci. USA* **107**, 1106-1111.
Heessen, S. and Fornerod, M. (2007). The inner nuclear envelope as a transcription factor resting place. *EMBO Rep.* **8**, 914-919.
Hershko, A. and Ciechanover, A. (1998). The ubiquitin system. *Annu. Rev. Biochem.* **67**, 425-479.
Hiller, M. M., Finger, A., Schweiger, M. and Wolf, D. H. (1996). ER degradation of a misfolded luminal protein by the cytosolic ubiquitin-proteasome pathway. *Science* **273**, 1725-1728.
Jentsch, S. and Rumpf, S. (2007). Cdc48 (p97): a 'molecular gearbox' in the ubiquitin pathway? *Trends Biochem. Sci.* **32**, 6-11.
Khmelinskii, A., Blaszczak, E., Pantazopoulou, M., Fischer, B., Omnus, D. J., Le Dez, G., Brossard, A., Gunnarsson, A., Barry, J. D., Meurer, M. et al. (2014). Protein quality control at the inner nuclear membrane. *Nature* **516**, 410-413.
Kolawa, N., Sweredoski, M. J., Graham, R. L. J., Oania, R., Hess, S. and Deshaies, R. J. (2013). Perturbations to the ubiquitin conjugate proteome in yeast deltaubx mutants identify Ubx2 as a regulator of membrane lipid composition. *Mol. Cell. Proteomics* **12**, 2791-2803.
Kostova, Z., Mariano, J., Scholz, S., Koenig, C. and Weissman, A. M. (2009). A Ubc7p-binding domain in Cue1p activates ER-associated protein degradation. *J. Cell Sci.* **122**, 1374-1381.
Kreft, S. G. and Hochstrasser, M. (2011). An unusual transmembrane helix in the endoplasmic reticulum ubiquitin ligase Doa10 modulates degradation of its cognate E2 enzyme. *J. Biol. Chem.* **286**, 20163-20174.
Krick, R., Bremer, S., Welter, E., Schlotterhose, P., Muehe, Y., Eskelinen, E.-L. and Thumm, M. (2010). Cdc48/p97 and Shp1/p47 regulate autophagosome biogenesis in concert with ubiquitin-like Atg8. *J. Cell Biol.* **190**, 965-973.
Ljungdahl, P. O. and Daignan-Fornier, B. (2012). Regulation of amino acid, nucleotide, and phosphate metabolism in *Saccharomyces cerevisiae*. *Genetics* **190**, 885-929.
Mannhaupt, G., Schnall, R., Karpov, V., Vetter, I. and Feldmann, H. (1999). Rpn4p acts as a transcription factor by binding to PACE, a nonamer box found upstream of 26S proteasomal and other genes in yeast. *FEBS Lett.* **450**, 27-34.
Mekhail, K. and Moazed, D. (2010). The nuclear envelope in genome organization, expression and stability. *Nat. Rev. Mol. Cell Biol.* **11**, 317-328.
Meyer, H., Bug, M. and Bremer, S. (2012). Emerging functions of the VCP/p97 AAA-ATPase in the ubiquitin system. *Nat. Cell Biol.* **14**, 117-123.
Mochida, K., Oikawa, Y., Kimura, Y., Kirisako, H., Hirano, H., Ohsumi, Y. and Nakatogawa, H. (2015). Receptor-mediated selective autophagy degrades the endoplasmic reticulum and the nucleus. *Nature* **522**, 359-362.
Neuber, O., Jarosch, E., Volkwein, C., Walter, J. and Sommer, T. (2005). Ubx2 links the Cdc48 complex to ER-associated protein degradation. *Nat. Cell Biol.* **7**, 993-998.
Omnus, D. J. and Ljungdahl, P. O. (2014). Latency of transcription factor Stp1 depends on a modular regulatory motif that functions as cytoplasmic retention determinant and nuclear degron. *Mol. Biol. Cell* **25**, 3823-3833.
Omnus, D. J., Pfirrmann, T., Andreasson, C. and Ljungdahl, P. O. (2011). A phosphodegron controls nutrient-induced proteasomal activation of the signaling protease Ssy5. *Mol. Biol. Cell* **22**, 2754-2765.

Pan, X., Roberts, P., Chen, Y., Kvam, E., Shulga, N., Huang, K., Lemmon, S. and Goldfarb, D. S. (2000). Nucleus-vacuole junctions in *Saccharomyces cerevisiae* are formed through the direct interaction of Vac8p with Nvj1p. *Mol. Biol. Cell* **11**, 2445-2457.

Park, S.-H., Kukushkin, Y., Gupta, R., Chen, T., Konagai, A., Hipp, M. S., Hayer-Hartl, M. and Hartl, F. U. (2013). PolyQ proteins interfere with nuclear degradation of cytosolic proteins by sequestering the Sis1p chaperone. *Cell* **154**, 134-145.

Pfirrmann, T., Heessen, S., Omnus, D. J., Andréasson, C. and Ljungdahl, P. O. (2010). The prodomain of Ssy5 protease controls receptor-activated proteolysis of transcription factor Stp1. *Mol. Cell. Biol.* **30**, 3299-3309.

Plemper, R. K., Bordallo, J., Deak, P. M., Taxis, C., Hitt, R. and Wolf, D. H. (1999). Genetic interactions of Hrd3p and Der3p/Hrd1p with Sec61p suggest a retro-translocation complex mediating protein transport for ER degradation. *J. Cell Sci.* **112**, 4123-4134.

Popken, P., Ghavami, A., Onck, P. R., Poolman, B. and Veenhoff, L. M. (2015). Size-dependent leak of soluble and membrane proteins through the yeast nuclear pore complex. *Mol. Biol. Cell* **26**, 1386-1394.

Prasad, R., Kawaguchi, S. and Ng, D. T. W. (2010). A nucleus-based quality control mechanism for cytosolic proteins. *Mol. Biol. Cell* **21**, 2117-2127.

Ravid, T. and Hochstrasser, M. (2007). Autoregulation of an E2 enzyme by ubiquitin-chain assembly on its catalytic residue. *Nat. Cell Biol.* **9**, 422-427.

Ravid, T. and Hochstrasser, M. (2008). Diversity of degradation signals in the ubiquitin-proteasome system. *Nat. Rev. Mol. Cell Biol.* **9**, 679-690.

Ravid, T., Kreft, S. G. and Hochstrasser, M. (2006). Membrane and soluble substrates of the Doa10 ubiquitin ligase are degraded by distinct pathways. *EMBO J.* **25**, 533-543.

Rendueles, P. S. and Wolf, D. H. (1988). Proteinase function in yeast: biochemical and genetic approaches to a central mechanism of post-translational control in the eukaryote cell. *FEMS Microbiol. Rev.* **4**, 17-45.

Roberts, P., Moshitch-Moshkovitz, S., Kvam, E., O'Toole, E., Winey, M. and Goldfarb, D. S. (2003). Piecemeal microautophagy of nucleus in *Saccharomyces cerevisiae*. *Mol. Biol. Cell* **14**, 129-141.

Romero-Perez, L., Chen, L., Lambertson, D. and Madura, K. (2007). Sts1 can overcome the loss of Rad23 and Rpn10 and represents a novel regulator of the ubiquitin/proteasome pathway. *J. Biol. Chem.* **282**, 35574-35582.

Rosenbaum, J. C., Fredrickson, E. K., Oeser, M. L., Garrett-Engele, C. M., Locke, M. N., Richardson, L. A., Nelson, Z. W., Hetrick, E. D., Milac, T. I., Gottschling, D. E. et al. (2011). Disorder targets misorder in nuclear quality control degradation: a disordered ubiquitin ligase directly recognizes its misfolded substrates. *Mol. Cell* **41**, 93-106.

Rubenstein, E. M., Kreft, S. G., Greenblatt, W., Swanson, R. and Hochstrasser, M. (2012). Aberrant substrate engagement of the ER translocon triggers degradation by the Hrd1 ubiquitin ligase. *J. Cell Biol.* **197**, 761-773.

Schork, S. M., Thumm, M. and Wolf, D. H. (1995). Catabolite inactivation of fructose-1,6-bisphosphatase of *Saccharomyces cerevisiae*. Degradation occurs via the ubiquitin pathway. *J. Biol. Chem.* **270**, 26446-26450.

Schuberth, C. and Buchberger, A. (2005). Membrane-bound Ubx2 recruits Cdc48 to ubiquitin ligases and their substrates to ensure efficient ER-associated protein degradation. *Nat. Cell. Biol.* **7**, 999-1006.

Schuberth, C. and Buchberger, A. (2008). UBX domain proteins: major regulators of the AAA ATPase Cdc48/p97. *Cell. Mol. Life Sci.* **65**, 2360-2371.

Schuberth, C., Richly, H., Rumpf, S. and Buchberger, A. (2004). Shp1 and Ubx2 are adaptors of Cdc48 involved in ubiquitin-dependent protein degradation. *EMBO Rep.* **5**, 818-824.

Sommer, T. and Jentsch, S. (1993). A protein translocation defect linked to ubiquitin conjugation at the endoplasmic reticulum. *Nature* **365**, 176-179.

Swanson, R., Locher, M. and Hochstrasser, M. (2001). A conserved ubiquitin ligase of the nuclear envelope/endoplasmic reticulum that functions in both ER-associated and Matalpha2 repressor degradation. *Genes Dev.* **15**, 2660-2674.

Thrower, J. S., Hoffman, L., Rechsteiner, M. and Pickart, C. M. (2000). Recognition of the polyubiquitin proteolytic signal. *EMBO J.* **19**, 94-102.

Tsuchiya, H., Arai, N., Tanaka, K. and Saeki, Y. (2013). Cytoplasmic proteasomes are not indispensable for cell growth in *Saccharomyces cerevisiae*. *Biochem. Biophys. Res. Commun.* **436**, 372-376.

Varshavsky, A. (2012). The ubiquitin system, an immense realm. *Annu. Rev. Biochem.* **81**, 167-176.

Walter, J., Urban, J., Volkwein, C. and Sommer, T. (2001). Sec61p-independent degradation of the tail-anchored ER membrane protein Ubc6p. *EMBO J.* **20**, 3124-3131.

Werner, E. D., Brodsky, J. L. and McCracken, A. A. (1996). Proteasome-dependent endoplasmic reticulum-associated protein degradation: an unconventional route to a familiar fate. *Proc. Natl. Acad. Sci. USA* **93**, 13797-13801.

Wójcik, C. and DeMartino, G. N. (2003). Intracellular localization of proteasomes. *Int. J. Biochem. Cell Biol.* **35**, 579-589.

Woolford, C. A., Daniels, L. B., Park, F. J., Jones, E. W., Van Arsdell, J. N. and Innis, M. A. (1986). The *PEP4* gene encodes an aspartyl protease implicated in the posttranslational regulation of *Saccharomyces cerevisiae* vacuolar hydrolases. *Mol. Cell. Biol.* **6**, 2500-2510.

Xie, Y. and Varshavsky, A. (2001). RPN4 is a ligand, substrate, and transcriptional regulator of the 26S proteasome: a negative feedback circuit. *Proc. Natl. Acad. Sci. USA* **98**, 3056-3061.

Zargari, A., Boban, M., Heessen, S., Andreasson, C., Thyberg, J. and Ljungdahl, P. O. (2007). Inner nuclear membrane proteins Asi1, Asi2, and Asi3 function in concert to maintain the latent properties of transcription factors Stp1 and Stp2. *J. Biol. Chem.* **282**, 594-605.

Supplemental Material

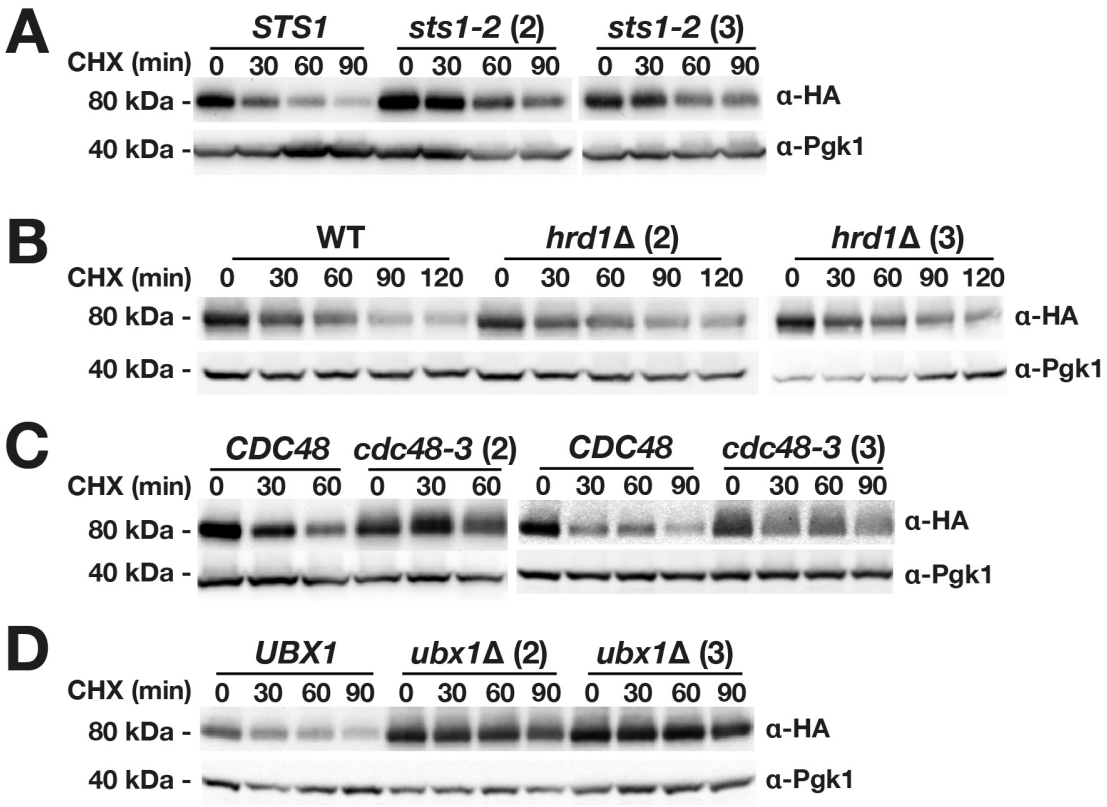

Figure S1. Replicate immunoblots used to quantitate the dependence of *STS1*, *HRD1*, *CDC48* and *UBX1* on Asi1 stability. (A) As in Fig. 2D (clone 1) - Asi1 is degraded in an *STS1*-dependent manner by proteasomes in the nucleus**.** The stability of Asi1 in *STS1* (NA10) and *sts1-2* (NA25) (independent clones 2 and 3) strains expressing Asi1-3HA (pPL1141). Cells were grown at 25 ^{o}C (permissive temperature) and shifted to 37 ^{o}C (non-permissive temperature) for 3 hours prior to CHX addition. **(B)** As in Fig. 4A (clone 1) - Asi1 turnover is independent of *HRD1*. CHX chase of Asi1-3HA (pPL1159) in WT (MBY154) and *hrd1*Δ (MBY155) (independent clones 2 and 3). **(C)** As in Fig. 5B (clone 1) - Asi1 turnover is impaired in *cdc48-3* temperature sensitive cells. CHX chase of Asi1-3HA (pPL1141) in *CDC48* (MHY1562) and *cdc48-3* (MHY3512) cells (independent clones 2 and 3). Cultures were grown at 25 ^{o}C (permissive temperature) and shifted to 37 ^{o}C (non-permissive temperature) 1 hour prior to CHX addition. **(D)** As in Fig. 5C (clone 1) - Asi1 turnover is impaired in *ubx1*Δ mutant cells. CHX chase of Asi1-3HA (pPL1141) in *UBX1* (BY4741) and *ubx1*Δ (BY4741$_{ubx1\Delta}$) cells (independent clones 2 and 3). Extracts from cells harvested at the indicated times were immunoblotted with anti-HA and anti-Pgk1.

Table S1. Yeast strains and plasmids used in this study

Strain	Genotype	Reference
CAY220	*MATα ura3-52 leu2Δ1 ssd1 cim3-1::RPT6*	(Pfirrmann et al., 2010)
MBY150	*MATα ura3-52 leu2-3,112 lys2Δ201 asi1Δ::kanMX*	This study
MBY151	*MATα ura3-52 leu2-3,112 lys2Δ201 asi1Δ::kanMX ubc6Δ::LEU2*	This study
MBY152	*MATα ura3-52 leu2-3,112 lys2Δ201 asi1Δ::kanMX ubc7Δ::LEU2*	This study
MBY153	*MATα ura3-52 leu2-3,112 lys2Δ201 asi1Δ::kanMX ubc6Δ::LEU2 ubc7Δ::natMX*	This study
MBY154	*MATα ura3-52 lys2Δ201 asi1Δ::kanMX*	This study
MBY155	*MATα ura3-52 lys2Δ201 asi1Δ::kanMX hrd1Δ::URA3*	This study
MBY156	*MATα ura3-52 lys2Δ201 asi1Δ::kanMX doa10Δ::natMX*	This study
MBY157	*MATα ura3-52 lys2Δ201 asi1Δ::kanMX doa10Δ::natMX hrd1Δ::URA3*	This study
PLY123	*MATα ura3-52 leu2-3,112 lys2Δ201*	Ljungdahl lab
PLY127	*MATα ura3-52 lys2Δ201*	Ljungdahl lab
PLY1314	*MATα ura3-52 asi1Δ::hphMX*	(Boban et al., 2006)
PLY1321	*MATα ura3-52 asi1Δ::hphMX asi3Δ::kanMX*	(Zargari et al., 2007)
PLY1327	*MATα ura3-52 lys2Δ201 asi1Δ::hphMX*	Ljungdahl lab
PLY1343	*MATα ura3-52 asi1Δ::hphMX asi2Δ::hisG*	(Zargari et al., 2007)
PLY1346	*MATα ura3-52 asi1Δ::hphMX asi2Δ::hisG asi3Δ::kanMX*	(Zargari et al., 2007)
PLY1348	*MATα ura3-52 leu2Δ1 ssd1 cim3-1*	(Pfirrmann et al., 2010)
PLY1581	*MATα ura3-52 trp1Δ101::loxP ASI3-6HA::Kl-TRP1*	Zargari et al., 2007)
PLY1630	*MATα ura3-52 asi1Δ::hphMX ssy5Δ::natMX,*	(Zargari et al., 2007)
PLY1811	*MATα ura3-52 lys2Δ201 ASI1-6HA::hphNT1*	This study
PLY1947	*MATα ura3-52 asi1Δ::hphMX asi2Δ::hisG asi3Δ::kanMX doa10Δ::natMX*	This study
YAZ101	*MATα ura3-52 lys2Δ201 asi1Δ::hphMX pep4Δ*	Ljungdahl lab
BY4741	*MAT***a** *his3Δ1 leu2Δ0 lys2Δ0 ura3Δ0*	M. Hochstrasser
$BY4741_{ubc7\Delta}$	*MAT***a** *his3Δ1 leu2Δ0 lys2Δ0 ura3Δ0 ubc7Δ*	M. Hochstrasser
$BY4741_{cue1\Delta}$	*MAT***a** *his3Δ1 leu2Δ0 lys2Δ0 ura3Δ0 cue1Δ*	M. Hochstrasser
$BY4741_{ubx1\Delta}$	*MAT***a** *his3Δ1 leu2Δ0 lys2Δ0 ura3Δ0 ubx1Δ*	M. Hochstrasser
MHY1562	*MAT***a** *his3Δ200 leu2-3,112 ura3-52 trp1 ade2-1*	(Ravid and Hochstrasser, 2007)
MHY3512	*MAT***a** *his3Δ200 leu2-3,112 ura3-52 trp1 ade2-1 cdc48-3*	(Ravid and Hochstrasser,

Strain	Genotype	Reference
		2007)
NA10	*MAT***a** *ura3-1 trp1-1 ade2-1 leu2-3, 112 his3-11 (STS1)*	(Chen et al., 2011)
NA25	*MAT***a** *ura3-1 trp1-1 ade2-1 leu2-3, 112 his3-11 sts1-2*	(Chen et al., 2011)
Plasmid	Description	References
pAZ013	pRS202 (2μ *URA3*) containing *ASI1*	Ljungdahl lab
pPL1136	pRS202 (2μ *URA3*) containing *ASI1-3HA*	(Zargari et al., 2007)
pPL1141	pRS316 (CEN/ARS *URA3*) containing *ASI1-3HA*	(Zargari et al., 2007)
pPL1142	pRS316 (CEN/ARS *URA3*) containing *3HA-ASI2*	(Zargari et al., 2007)
pPL1159	pRS317 (CEN/ARS *LYS2*) containing *ASI1-3HA*	Ljungdahl lab
pPL1307	YEp195-based (2μ *URA3* replaced with *LYS2*) containing P_{CUP1}-*6HIS-UBI*	(Omnus et al., 2011)